Atmos. Meas. Tech. Discuss., 7, 9869–9915, 2014
www.atmos-meas-tech-discuss.net/7/9869/2014/
doi:10.5194/amtd-7-9869-2014

Atmospheric Measurement Techniques Discussions
Open Access

Observations of precipitable water vapour over complex topography of Ethiopia from ground-based GPS, FTIR, radiosonde and ERA-Interim reanalysis

G. Mengistu Tsidu[1,2], **T. Blumenstock**[2], **and F. Hase**[2]

[1]Department of Physics, Addis Ababa University, P.O. Box 1176, Addis Ababa, Ethiopia
[2]Karlsruhe Institute of Technology (KIT), Institute for Meteorology and Climate Research (IMK-ASF), Karlsruhe, Germany

Received: 29 April 2014 – Accepted: 8 September 2014 – Published: 23 September 2014

Correspondence to: G. Mengistu Tsidu (gizaw_mengistu@gmx.net)

Published by Copernicus Publications on behalf of the European Geosciences Union.

Abstract

Water vapour is one of the most important green house gases. Long-term changes in the amount of water vapour in the atmosphere need to be monitored not only for its direct role as a green house gas but also because of its role in amplifying other feedbacks in general circulation models. In recent decades, monitoring of water vapour on regular and continuous basis is becoming possible as a result of increase in the number of deployed Global Positioning Satellite (GPS) ground-based receivers at a faster pace. However, Horn of Africa region remains a data void region in this regard until recently when some GPS ground-receiver stations have been deployed to monitor tectonic movements in the Great Rift Valley. This study seizes this opportunity and the installation of Fourier Transform Infrared Spectrometer (FTIR) at Addis Ababa to assess the quality and comparability of Precipitable Water Vapour (PWV) from GPS, FTIR, radiosonde and ERA-Interim over Ethiopia. The PWVs from the three instruments and reanalysis show good correlation in the range from 0.83 to 0.92. The radiosonde PWV shows dry bias with respect to other observations and reanalysis. ERA-Interim PWV shows wet bias with respect to all while GPS PWV exhibits wet bias with respect to FTIR. The intercomparison between GPS and ERA-Interim is extended to seven other GPS stations in the country. Despite the sensitivity of GPS PWV to uncertainty in surface pressure in general, observed surface pressure is used only at four GPS stations. The gain obtained from using observed surface pressure in terms of reducing bias and strengthening correlation is significant but shows some variations among the GPS sites. In contrast to comparison at Addis Ababa, the comparison between GPS and ERA-Interim PWVs over seven other GPS stations shows difference in the magnitude and sign of bias of ERA-Interim with respect to GPS PWV from station to station. This variation is also visible across different seasons. The main cause of the variation is linked to variation in ECMWF model skill over different regions and seasons which might be related to poor observational constraint from this part of the globe and sensitivity of model convection scheme to orography. The latter is consistent with observed

AMTD
7, 9869–9915, 2014

wet bias over some highland stations and dry bias over few lowland stations. However, there are also exceptions to this inference at few stations suggesting other factors such as proximity to water bodies and vegetations might have a role. The skill of ECMWF in reproducing realistic PWV varies with season showing large bias during warm and wet summer for most of the GPS sites.

1 Introduction

Drought and floods represent climate hazards that can cause great damage in terms of human suffering and losses on every sector of the economy. Both can be traced in terms of the analysis of water vapour cycles in the atmosphere. Water vapour is one of the most important greenhouse gases. Long-term changes in the amount of water vapour in the atmosphere need to be monitored as part of an effort to understand and predict impending climate change. Water vapour in the atmosphere is a parameter of great importance in climate models because of its role as a greenhouse gas. In fact, water vapour is a very efficient greenhouse gas. Some studies have suggested that a substantial increase in water vapour content in the tropics could give a larger impact than a doubling of the carbon dioxide concentration (Buehler et al., 2006; Nilsson and Elgered, 2008). It acts also to amplify other feedbacks in general circulation models, such as cloud and albedo feedbacks. On longer time scales, water vapour changes are thought to contribute to an important positive feedback mechanism for climate change. Warming of the surface, particularly the sea surface, leads to enhanced evapouration. Due to the fact that water vapour is a greenhouse gas, enhanced water vapour in the lower troposphere results in further warming, allowing a higher water vapour concentration, thereby creating a positive feedback. An increase of temperature can result in an increase in total precipitable water vapour (PWV) since the equilibrium vapour pressure increases with increasing temperature. Mears et al. (2007) have determined that an increase of the temperature of 1 K will result in a 5–7 % rise in PWV. It is also

AMTD
7, 9869–9915, 2014

suggested that long time series of PWV measurements can be used as an independent data source to detect global warming.

Atmospheric water vapour exhibits substantial diurnal variations (e.g. Dai and Hove, 2002; Wang et al., 2007, and references therein). These variations affect surface and atmospheric longwave radiation and atmospheric absorption of solar radiation as well as other processes, such as diurnal variations in moist convection and precipitation, surface wind convergence and surface evapotranspiration. Unfortunately, there is a lack of data with high temporal resolution for studying the diurnal cycle of water vapour on the global scale. Therefore one of scientific objectives for creating a global water vapour data set using high-temporal-resolution Global positioning satellite (GPS) measurements is to analyze the data to document and understand water vapour diurnal variations, and to validate the representation of the water vapour diurnal cycle in climate and weather models.

One way to monitor water vapour is measurements of precitable water (PWV) using various instrumentations onboard different platforms. PWV measurements can also be used to understand weather and improve forecasting as it is a crucial element in clouds and precipitation development. In the past, weather service centers relied on information from radiosonde launches and satellite to have first order estimate of the humidity distribution. However, the density of radiosonde is very sparse and nonuniform often related to running costs. As a result, it is rare to find more than a site per country over many parts of the globe and the situation is worse in Africa. Moreover, sustainability of the radiosonde sites has been a challenge which has been reflected in data gaps in historical time series and interruption in data transmission to world meteorological (WMO) data centers for operational global use. Furthermore, water vapour observation from radiosonde can not capture rapid changes due to slow ballon ascent. On the other hand, satellite observations do not suffer from such problems. However, the PWV estimate from satellites is complicated over land due to surface temperature variability.

In recent decades, the use of GPS has been extended to investigation of the upper and lower atmosphere. GPS can provide a high resolution continuous measurement of

AMTD
7, 9869–9915, 2014

zenith tropospheric delay from which a near real-time total precipitable water vapour around a ground GPS-receiver site can be derived. In view of increase in the number of GPS-receiver sites globably for use in areas ranging from survey to geodetic investigation and their use across disciplines, a number of studies have explored the potential use of GPS for lower atmosphere research. Moreover, apart from continuity and high temporal resolution, a GPS receiver can run automatically once installed. One of the scientific objectives of creating a global PW data set from GPS measurements is to take advantage of the increasing volume and maturity of GPS data and more importantly its long-term stability. To this end, considerable efforts have been devoted to derive PWV using ground-based GPS measurements (e.g., Bevis et al., 1992, 1994; Rocken et al., 1993, 1997) at high temporal resolutions, validating radiosonde, satellite and reanalysis data (e.g., Yang et al., 1999; Guerova et al., 2003; Dietrich et al., 2004; Van Baelen et al., 2005; Bock et al., 2010; Schneider et al., 2010; Buehler et al., 2012), improving numerical weather prediction (e.g., Vedel and Huang, 2004; Vedel et al., 2004; Gendt et al., 2004), creating near global and high temporal PWV datasets for monitoring climate change and variability (e.g., Gradinarsky et al., 2002; Wang et al., 2007, 2009). Some studies have investigated the possibility to quantify the precipitable water vapour in the line of sight of the GPS satellite (e.g., Braun et al., 2003; Champollion et al., 2005, and references therein) which then can be used to study the 3-D heterogeneity of the troposphere based on tomographic methods.

Despite considerable exploitation of steadily expanding multi-purpose ground-based GPS receiver networks for investigation of water vapour variability and climate change globally, the same experiences were not replicated over Africa due to lack of GPS network with exceptions over southern Africa region (e.g., Combrink et al., 2004, and references therein). Most efforts to validate satellite and model estimates of precipitable water over Africa are hindered due to lack of GPS and other ground based atmospheric observing systems and show large data gaps (e.g., Fetzer et al., 2003; King et al., 2003; Bock et al., 2007).

AMTD
7, 9869–9915, 2014

However, recent increase in the number of GPS ground receiver sites for geodetic studies over North Africa and AMMA project over west Africa has initiated assessment of water vapour content over these regions (Bock et al., 2007; Koulali et al., 2011). For instance, Koulali et al. (2011) have used GPS PWV and other complimentary observations to show that the monthly mean precipitable water variation over Morocco is controlled by the upper layer zonal and meridional moisture flux. Bock et al. (2007) have used some scattered GPS receiver stations over Africa and compared to independent observations, ERA-40 and NCEP2 model simulations. While these studies hardly represent the whole of Africa, they are steps in the right direction to fill the existing data gaps and understanding of water vapour variability. However, there is no similar work over the Eastern Africa Rift Valley region, a region with almost no observations until recently. A number of GPS sites are installed since 2007 to monitor geodetic activity either in campain mode or as a permanent stations along the Great Rift Valley regions and adjoining Ethiopian highlands. Most of these stations are still operating and providing data albeit some interruption at some stations. The use of the data from these stations for investigating PWV over this region is of a considerable interest not only because of existing data gaps but also because of the fact that the region has exeprienced recurring droughts for the last two decades which is not yet fully understood. The GPS derived PWV can compliment existing data to understand climate change and variability and their links to the recurring droughts. In this work, intercomparisons of PWVs from GPS, Fourier Transform Spectrometer, radiosonde and ERA-Interim are made. The agreements between the various datasets and spatial and seasonal disparties are investigated.

The paper is outlined as follows. In Sect. 2, data and the methodology used in this work are presented. Results and discussion are given in Sect. 3 and finally conclusions are given in Sect. 4.

AMTD
7, 9869–9915, 2014

2 Data and methodology

The observations of atmospheric precipitable water vapour over Addis Ababa are performed using ground-based GPS receivers, Fourier Transform Infrared Spectrometer (FTIR), and radiosonde. Radiosonde observation is a daily observation carried out at Addis Ababa synoptic meteorological station for long time despite gaps due to measurement interruption, failed launches and problems with data quality. FTIR was installed in May 2009 and monitors most atmospheric trace gases by recording solar absorption spectra. Ground GPS receivers are installed not only in Addis but also along the Ethiopian Rift Valley and neigbouring highlands as part of monitoring tectonic movement at different times over the last few years. ERA-Interim PWV is found to capture the truth elsewhere from previous studies (e.g., Bock et al., 2005, 2007; Koulali et al., 2011) which is less complex in terms of topography as compared to East Africa. This encouraged us to use ERA-Interim PWV in this study to know how good it is over Ethiopia. In the following, the respective data sets and methodolgies used in acquiring them from these instruments and for intercomparison are described.

2.1 FTIR observations

The Addis Ababa FTIR site is a tropical high latitude site with geocoordinate at 9.01° N latitude, 38.76° E longitude, 2443 m altitude a.s.l. Our FTIR instrument is a commercial Bruker IFS-120MR spectrometer. Two detectors, mercury-cadmium-telluride (Hg-Cd-Te) and indium-antimonide (InSb) detectors, allow wider spectral coverage and enable retrieval of several trace species (Takele Kenea et al., 2013).

The retrieval of atmospheric trace gases from measured spectra is nearly a subset of the spectral microwindows used by Schneider et al. (2012). The retrieval method is a sequencial procedure in which solar lines are first retrieved, which is then used in the subsequent retrieval of water vapour. These results are both used in following retrievals of N_2O, CH_4, O_3 and other gases. Daily pressure and temperature vertical profiles used to evaluate the FTIR data were taken from the automailer system of Goddard Space

AMTD
7, 9869–9915, 2014

Flight Center. The climatological profiles were based on data from the National Center for Environment Prediction (NCEP). The retrieved state vector contains the retrieved volume mixing ratios of the target gas defined at 44 levels in the atmosphere, as well as the retrieved interfering species column amounts, and fitted values for some model parameters. These can include the baseline slope and instrumental lineshape parameters (Hase et al., 1999). The retrieval of H_2O volume mixing ratio (VMR) is performed on a logarithmic scale because of large vertical dynamic range and high variablity near the boundary layer. The spectral microwindows used for the water vapour retrieval include seven spectral ranges in the mid-infrared shown in Table 1. Table 1 also shows the interfering species jointly retrieved with water vapour.

The retrieved water vapour profiles are characterized in terms of its information content based on degrees of freedom, vertical resolution and different error sources following optimal estimation method (Rodgers, 1976, 2000).

2.2 GPS observations

The zenith tropospheric delay can be estimated from measurements of the delay to each GPS satellite in view from a ground station. Signal from several GPS satellites, up to 9 to 11, can be received at any given time over a given GPS ground receiver site. However, a network of ground GPS receivers are required to determine GPS orbits and several biases due to satellite clocks, receiver clocks, and receiver biases. The analysis of GPS data obtained at such network produces an estimate of total tropospheric zenith delay (TZD) which can be splitted into dry hydrostatic (ZHD) and wet zenith (ZWD) delays. The ZWD is that part of the range delay that can be attributed to the water vapour in the troposphere. ZWD can be determined from TZD GPS measurement and ZHD corrected a priori using Saastamoinen (1972) formula.

If the vertically integrated water vapour overlying a reciever is stated in terms of PWV, then this quantity can be related to the ZWD at the receiver by

$$\mathrm{PWV} = \pi \times \mathrm{ZWD}, \quad (1)$$

AMTD
7, 9869–9915, 2014

where the ZWD is given in units of length, and the dimensionless constant of proportionality π is a function of T_m given by an empirical model

$$\pi = \frac{10^6}{\rho R_v \left[\left(\frac{k_3}{T_m}\right) + k_2'\right]} \quad (2)$$

where ρ is the density of liquid water, R_v is the specific gas constant for water vapour, k_3 and k_2' are constants with values of 3700 $K^2\,Pa^{-1}$ and 0.22 $K\,Pa^{-1}$ respectively, and T_m is a weighted mean temperature of the atmosphere. T_m is usually given in terms of surface temperature as

$$T_m = a \times T_s + b,$$

where $a = 0.72$ and $b = 70.2$ were estimated using radiosondes data within the United States (Bevis et al., 1994). The coefficients vary with season and latitude. Therefore. we used T_m estimates computed from temperature and humidity profiles of ECMWF and made available at the technical university of Vienna (http://ggosatm.hg.tuwien.ac.at/DELAY/).

The GPS data are processed with GAMIT software package v10.32 (King and Bock, 2006), which solves the tropospheric and other parameters using a constrained least squares algorithm. The input data required by GAMIT are the raw GPS observations, earth orientation parameters, and two-hour orbit predictions from the hourly GPS satellite orbit product generated by the Scripps Orbit and Permanent Array Center (SOPAC). The software is based on a method referred to as a network solution in which several sites are processed together. ZWD is modeled as a piecewise linear function of time with the nodes being parameterized as first order Markov process with a standard deviation of 0.02 $m\,h^{-\frac{1}{2}}$. The ZWD estimates are the nodes of the Markov process and are estimated every 2 h along with tropospheric gradient parameters. The Global Mapping Function (Boehm et al., 2007) was used for mapping ZHD and ZWD into the slant path directions of the GPS satellites at each epoch. The Vienna Mapping Function based

AMTD
7, 9869–9915, 2014

on exact ray traces through the refractivity profiles of a ECMWF data at 3° elevation is used. The elevation cut-off angle was fixed to 10°. This translates to a radius of about 28 km at an altitude of 5 km (note that most water vapour is found with the first 5 km layer). This implies that GPS ZWD is close to that of a purely vertical integral measurement and hence it can represent PWV at ground-based GPS receiver location. The GPS data were processed in double-difference mode in 24 h observing sessions within the University NAVstar COnsortium (UNAVCO) network in the region shown in Fig. 1. The precipitable water vapour (PWV) is determined from GPS ground receivers installed along and across the Rift Valley. GPS stations installed along the main Rift system over Ethiopia consists of Semera in the North, Nazerate in the centre and Arbaminch in the South while those installed across the Rift systems include Robe in the southern highlands, Addis Ababa in the central highlands, Alemaya in the southeastern highlands, Mekele in the northern highlands and BahirDar in the northwestern highlands of the country as indicated in Fig. 1 (right panel). The PWV is derived for the 2007–2011 period with some data gaps in between at all stations but at different times as indicated in Table 3. There are also some GPS ground receiver stations with large data gaps and some of which are not working anymore. The above eight GPS stations are selected for further analysis as they represent different climate regimes over the country (Mengistu Tsidu, 2012).

In the absence of in situ meteorological data, the best choice of pressure and temperature for a site comes from the global pressure and temperature (GPT) model (Boehm et al., 2007). Since, we have surface observations at only four of the eight GPS stations (see Table 2), we used GPT as well as observed pressure and temperature. The difference between PWV estimates based on presure and temperature from GPT model and observation is used to assess the performance of GPT model and to evaluate the risk of using them in places where observations are not available in the country.

AMTD
7, 9869–9915, 2014

2.3 Radiosonde soundings

The radiosonde sounding data for synoptic meteorological station is taken from Integrated Global Radiosonde Archive (IGRA) at the National Climatic Data Center (NCDC). The IGRA archive contains quality-assured data (Durre et al., 2006). However, IGRA does not include correction or data gap filling and in effect, the archive contains a lot of missing values and only a relatively small number of observations are used in the intercomparison despite the daily radiosonde sounding is a long time series. Dew point temperature is computed from dew point depression and temperature sounding which is then used to determine vapour pressure. The vapour pressure along with surface pressure are used to compute specific humidity. The precipitable water vapour (PWV in units of cm) is then determined from

$$\mathrm{PWV} = \frac{1}{g_\mathrm{o}} \int_{p_\mathrm{o}}^{p_\mathrm{surf}} q(p)\mathrm{d}p \tag{3}$$

where $q(p)$, the specific humidity as a function of atmospheric pressure p, is given in units of $\mathrm{g\,kg^{-1}}$ and $g_\mathrm{o} = 980.665\,\mathrm{cm\,s^{-2}}$.

2.4 ERA-Interim data

ECMWF is currently providing ERA-Interim based on cycle 31r2 of the Integrated Forecasting System (IFS). Relative to the ERA-40 system, which was based on IFS cycle 23r4, ERA-Interim incorporates many important IFS improvements such as model resolution and physics changes, the use of four-dimensional variational data assimilation (4-D-Var), and various other changes in the analysis methodology (Dee et al., 2011). The precipitable water vapour from reanalysis dataset has been found to be in good agreement with in-situ and GPS observations, in particular, good agreement between ERA-40 PWV and GPS PWV at some GPS sites in West and North Africa (Bock et al., 2007).

AMTD
7, 9869–9915, 2014

The vertical interpolation of PWV from ERA-Interim grid to GPS site is computed based on

$$\Delta\mathrm{PWV} = \rho_v \Delta h (1 - \frac{\rho_v \Delta h}{2\mathrm{PWV}}) \quad (4)$$

where ρ_v is water vapour density and Δh and ΔPWV are altitude and PWV differences respectively between ERA-Interim nearest grid and GPS site as proposed by Bock et al. (2007). Since, we have used the high resolution version of ERA-Interim, the correction made in this manner is insignificant as it will be shown later.

3 Results and discussion

3.1 Data quality

3.1.1 Characterization of water vapour VMR from FTIR

The retrieval of vertical profile of trace gases from ground-based FTIR spectra depends on the sensitivity of the absorption lines to pressure broadening such that the spectral line centers provide information about distribution of trace gases at higher altitudes while the wings of a line give information at the lower altitudes. This entails that the information content of the retrieval will strongly depend on the choice of the absorption lines and use of fairly accurate pressure and temperature profiles. As we have noted the spectral microwindows used are subset of the microwindows used by Schneider et al. (2012) and under efforts are underway to make them standard for NDACC community. The pressure and temperature profiles are taken from NCEP which also provides pressure and temperature profiles to other NDACC sites. However, the contribution of pressure and temperature uncertainty to the over all error budget in retrieval of trace gases from FTIR absorption spectra is insignificant.

The trace of the averaging kernel matrix, the degrees of freedom for signals, is a useful metric to characterize the retrieval of water vapour. It represents the number of

AMTD
7, 9869–9915, 2014

independent pieces of information retrieved from the measurements. The degrees of freedom vary between 1.6 and 2.0 (Fig. 2) suggesting existence of about 2 independent layers. This is within the values found by others (e.g., Schneider et al., 2006) though further mariginal improvement can be achieved with longer integration time.

The retrieval of water vapour VMR can also be characterized by assessing the different errors sources such as temperature, noise, instrumental line shape, solar lines, line of sight, baseline, and spectroscopy. However, what is interesting in the context of this study is to investigate how the total error due to uncertainty in these parameters affects the PWV. Figure 3 shows precipitable water vapour (panel a) and statistical error (panel b) and systematic error (panel c) in PWV for all measurements. The statistical error in PWV is considerably small and remains lower than 0.1 mm throughout most of the measurements. The systematic error varies between 0.2 to 0.6 mm for most of the observations with exception exceeding 0.6 mm in few cases. The error estimation is based on the widely used method (e.g., Takele Kenea et al., 2013, and references therein) as suggested by Rodgers (2000).

3.1.2 GPS PWV quality

GPS as a water vapour observing technique is quite recent, but it has proven to be as accurate as conventional techniques (e.g., Bevis et al., 1992; Klein Baltink et al., 2002). In contrast to the radiosonde data, the ground-based GPS data have not yet been assimilated in the reanalysis output (e.g., ECMWF ERA-Interim which is used in this work). In this respect, GPS PWV can serve as an independent validation data set suitable for the evaluation of reanalysis (e.g., Bock et al., 2007 and references therein) and climate models (Ning et al., 2013). To serve in all these tasks, a formal quality assessment should be performed. The quality of GPS PWV can be assessed from estimation error of PWV from GPS observable. The GPS PWV are processed in 24 h observing sessions at an interval of 2 h. The inspection of estimation error shows an increase in scatter at 00:00 UTC for all eight GPS sites. This has been also reported by Bock et al. (2008). Figure 4 shows estimation error in PWV for all observations. The

AMTD
7, 9869–9915, 2014

estimation error for Addis Ababa site (Fig. 4a) remains lower than 2 mm during most of the time. However, there are also higher values which are filtered out on some occassions. Similar error pattern was also observed for Bahir Dar GPS site (Fig. 4b) except some observation gaps. Estimation error at most of the remaining GPS sites (Fig. 4c–h) is in the order of 1.2 mm on average with different size of data gaps between the GPS sites. We have also estimated the error propagation from uncertainity in zenith path delay, surface pressure and atmospheric mean temperature to PWV from the theoretical and empirical relationships used in the linear least squares solutions assuming uncertainty of 4 mm in zenith path delay, 1.65 hPa in surface pressure and 1.3 K in mean atmospheric temperature as described by Wang et al. (2007) for Addis Ababa GPS site. We found that these uncertainties contribute about 1.32 mm in agreement with finding of Wang et al. (2007).

On the other hand, assumption of only 1.65 hPa surface pressure uncertainty is not realistic when the surface pressure from global pressure-temperature model (GPT) or reanalysis such as ECMWF is used in estimation of PWV from GPS zenith path delay. For instance, we found between 1 to 10 hPa difference for 4 of the GPS stations with surface pressure measurements within a radius of 50 km. We have investigated the impact of possible inaccuracy of GPT data used in our study using surface pressure measurements from nearby synoptic stations within the 50 km radius after accounting for altitude difference between synoptic and GPS stations by vertically interepolating the surface pressure measurements following procedure proposed by Wang et al. (2007) for Addis Ababa, Bahir Dar, Mekele and Nazerate. The vertically interpolated surface pressure is used to estimate the zenith hydrostatic delay which is used along with the estimated ZTD to determine the ZWD from which PWV is evaluated according to Eq. (1). While the data gaps in surface measurements dramatically reduced the number of the obseravtions available for comparison with other instruments and reanalysis, the bias in the GPS PWV has been reduced significantly as will be discussed later.

AMTD
7, 9869–9915, 2014

3.1.3 Radiosonde PWV

PWV depends on both temperature and humidity. Therefore, measurement errors affecting them are source of uncertainty in radiosonde-based PWV. The slow response in humidity sensors and radiation exposure related to temperature sensors at many stations in the past were sources of problems. Various methods have been developed to correct known humidity observational errors for individual type of radiosonde within a region through either statistical approaches (Turner et al., 2003; Voemel et al., 2007) or laboratory or physical correction schemes. The radiosonde data from Addis Ababa synoptic meteorological station has undergone quality checks by IGRA through scrutinizing presence of physically implausible values, internal inconsistencies among variables, climatological outliers, and temporal and vertical inconsistencies in temperature (Durre et al., 2006).

The type of radiosonde used is Vaisala RS92 and the measurement, which is carried out once per day, is taken at 12:00 UTC. Bias correction of different radiosondes has been reported for different radiosonde types (e.g. Agusti-Panareda et al., 2009, and references therein). Vaisala RS92 is found to be the most accurate from the Atmospheric Infrared Sounder (AIRS) Water Vapour Experiment (AWEX) as demonstrated by mean percentage accuracy within 5–10 % in lower to upper troposphere relative to Cryogenic Frostpoint Hygrometer (Miloshevich et al., 2006).

3.1.4 ECMWF ERA-Interim PWV

The quality of the model simulated precipitable water vapour has been assessed for the ECMWF reanalysis products. For older versions of reanalysis (e.g., ERA40), Trenberth et al. (2005) found that the values are reasonable over land as demonstrated by good agreement with radiosondes but with relatively large errors over oceans. For the latest ERA-Interim that is used in this work, the agreement with observations is significantly improved for most variables (Paul Berrisford et al., 2009; Dee et al., 2011). COSMIC observations are assimilated in ERA-Interim reanalysis beginning December 2006,

AMTD
7, 9869–9915, 2014

however, due to unavailability of ground-based GPS observations until recently, data from this part of the globe is neither assimilated in models or used for any intercomparison or validation purpose. This has been noticed indirectly from large discrepancy found in recent comparison of ECMWF precipitation with observations (Mengistu Tsidu, 2012). Nevertheless, in a broader context and global picture, ECMWF analysis provides optimal humidity estimates from high quality observations among multi-satellite sounders, imagers, and radiosondes through a data assimilation system. The data quality is granted through consistency checks among observational data sources used in the assimilation through a series of adaptive bias correction and quality control procedures (Auligne et al., 2007).

3.2 Intercomparison of PWVs from different instruments and reanalysis over Addis Ababa

We use Addis Ababa as a case study to demonstrate the reliability of PWVs from GPS, FTIR, radiosonde and ECMWF ERA-Interim and their consistency with each other since FTIR and GPS are colocated at Addis Ababa geophysical observatory and the daily radiosonde data from the Addis Ababa synoptic station is only about 4 km away at an altitude lower than this site by approximately 80 m. Moreover, the radiosonde is part of the global data set assimilated in the ECMWF ERA-Interim model.

Figure 5 shows comparison of radiosonde and GPS PWVs determined based on GPT surface pressure (panel a) and observed surface pressure (panel b) at Addis Ababa site at 12:00 UTC as described in Sect. 2.2. There is considerable improvement in the agreement of the two data sets as reflected in sharp drop in the wet bias from about 3 mm in GPS PWV with respect to radiosonde when GPT is used (Fig. 5a) to nearly zero after observed surface pressure is employed (Fig. 5b). However, the correlation did not show significant improvement suggesting that inaccuracy in surface pressure used in GPS PWV processing affects the magnitude not the phase of the variation as it is part of a systematic error. It has been known from several previous studies that PWV from radiosonde is generally dry biased at the upper ends of PWV time series as

AMTD
7, 9869–9915, 2014

reflected in Fig. 5. Almost identical coincident ERA-Interim PWV comparison with radiosonde exhibits dry bias in radiosonde as shown in Fig. 6. Note that Fig. 6 represents ERA-Interim and radiosonde association with correction of the altitude difference between nearest ECMWF grid from which ERA-Interim PWV is extracted and GPS site. The applied correction is minor due to proximity of the high resolution model grid (i.e. $0.75^{\circ} \times 0.75^{\circ}$ horizontal resolution) to Addis Ababa GPS site.

The dry bias is also consistently observed with respect to ERA-Interim but the dry bias is much larger in this case. This is not surprising since models in general including high resolution regional models (e.g., Zeleke et al., 2013) and ERA-Interim in particular show wet bias over high altitude regions of Ethiopia (Mengistu Tsidu, 2012) as a result of high sensitivity of their convection schemes. While this difficiency is generally common to all high latitude regions, the major problem which is more specific to the region is lack of observations that would have been assimilated into the model for a better results.

We have also FTIR observations at the observatory which could have been compared to radiosonde. However, FTIR instrument measures solar radiance after attunation by atmospheric constitutent present along the line of sight and therefore operates under clear sky and sunny conditions with no clouds along the line of sight. As a result, FTIR is limited to daytime observation when the sun is at sufficiently high zenith angle beyond any physical ground obstruction in the direction of line of sight. Moreover, clear conditions limit the observation period to be seasonal with more observations during relatively dry and clear sky. In addition, due to various technical issues, the FTIR observations were not continuous enough even under the physical limitations stated above. Due to these and large gaps in the daily radiosonde observations, it was not possible to find data sets that meets the 1 h interval of coincident observations.

On the other hand, since GPS PWV is estimated at an interval of 2 h and ERA-Interim is given at a temporal resolution of 6 h, it was possible to find FTIR-GPS and FTIR-ERA-Interim coincident measurements as shown in Fig. 7. Despite, GPS PWV is estimated at higher temporal resolution than ERA-Interim, the number of coincident

AMTD
7, 9869–9915, 2014

data points between FTIR and ERA-Interim is three-fold larger than that of FTIR and GPS observations. This is also attributable to the sizable data gaps in GPS observations in contrast to regular reanalysis data. The correlation of FTIR and GPS PWVs is 0.92 and GPS has a wet bias of up to 0.6 mm whereas the correlation between FTIR and ERA-Interim is 0.83 with a bias of 1.6 mm. Even though these coincident observations are different from those observations in Figs. 5 and 6, there is evidence for wet bias in ERA-Interim consistently against all observations from other instruments. Moreover, GPS PWV shows also a wet bias against both radiosonde and FTIR PWVs at the higher ends of the PWVs. While it is generally understood the wet bias in GPS PWV with respect to radiosonde arises from known sensor caliberation problems in the radiosonde data set globally that tend to underestimate PWVs, it is not clear about the wet bias in GPS PWV with respect to FTIR at the higher ends of PWV values. A single previous similar study at Izana observatory shows rather dry bias in GPS as compared to FTIR at lower ends of PWV values (Schneider et al., 2010). We need to caution that Izana is generally dry compared to Addis Ababa from comparison of their analysis and our results.

The correlations in PWVs from the three observations and reanalysis model at Addis Ababa imply strong correlation despite wide range of variation in PWV in the area. The biases in the respective data sets with respect to each other consistently show the same directions regardless of difference in the data used for each pair involving instruments and/or reanalysis. This assessment is in agreement with previous similar studies as well as different but related investigations over the region. The error characterization, data quality and consistency of the PWV observations from different instruments and reanalysis can build our confidence in the data sets from the region far away from Addis Ababa site. This is indeed important to establish as we do not have many coincident instrumentations elsewhere in the region. Radiosonde at Addis Ababa is a sole radiosonde observation in the whole of Ethiopia whereas FTIR is a unique and only facility in the whole of continental Africa. Therefore, GPS observations at other sites and ECMWF ERA-Interim reanalysis in the region are the only observations that provide

AMTD
7, 9869–9915, 2014

PWV from ground. The reliability of GPS PWVs depends on availability of surface pressure observations and on how close the surface pressure used from GPT model in the absence of observations. The wet bias observed in ERA-Interim PWVs may not be the same everywhere in the region. We have used surface pressure observations to determine GPS PWVs whereever possible in spite of large data gaps in some cases. Thus, our analysis and interpretation in the following sections are made in the context of agreement between the two data sets and other indirect investigations wherever available.

3.3 Comparison of PWVs from GPS and ERA-Interim reanalysis at other sites in Ethiopia

As stated earlier, similar assessment can not be made at other sites since radiosonde and FTIR observations at Addis Ababa are the only available facilities in the country. Moreover, lack of availability of synoptic meteorological stations close to some of other GPS sites, namely Semera, Alemaya, Arbaminch, and Robe, used in this study forced us to rely on other indirect studies to understand the agreement between the GPS and reanalysis. In addition, the level of correction made to GPS PWVs observations at Addis Ababa, Mekele, Bahir Dar and Nazerate from using surface pressure observations can also give clues as to whether we need to be worried at other sites where the corrections are not made. Figure 8 shows comparison of ERA-Interim and GPS PWVs for eight stations including Addis Ababa for all coincident observations from 2007–2011. As we have indicated in the preceding section the GPS data has gaps of different sizes. For instances observations at Mekele is less than a year taken only in 2008. Observations at Alemaya, Semera and Robe span only three years from 2007–2009 with gaps in between while observations at Addis Ababa, Nazerate, Bahir Dar and Arbaminch cover the period from 2007 to 2011 with also varying degree of data gaps (see Table 3). Furthermore, sparsity in data exhibited at Addis Ababa, Nazerate, Mekele and Bahir Dar is due to exclusion of observations where corresponding surface

AMTD
7, 9869–9915, 2014

observations are either unavailable or not recommended according to NOAA NCDC data quality flag.

Figure 8 (top-left) shows ERA-Interim vs. GPS PWVs at Addis Ababa GPS site covering all data where correction can be made as a result of available surface observations. The wet bias in ERA-Interim PWV with respect to GPS increases while the correlation is about 0.85. The wet bias is throughout the whole range of PWV values with minor enhancement at the higher ends of PWV values.

Figure 8 (top-right) shows ERA-Interm vs. GPS PWVs determined based on surface synoptic meteorological observations at Nazerate ground GPS receiver site. What is distinct in this case is dry bias in ERA-Interim PWV. As revealed in our investigation in Sect. 3.2, the PWVs from GPS show better agreement with FTIR and radiosonde than reanalysis. Therefore, the dry bias in ERA-Interim must be inherent in the reanalysis data itself than associated with possible wet bias in GPS PWV as a result of poor performance of GPS itself. The dry bias in ERA-Interim reanalysis may not be solely attributed to sensitive convection parameterization to topography in the ECMWF model because this site is on the escarpment of the Rift Valley located at a height of 1722 m a.s.l. which is high enough to induce wet bias contrary to what is seen in ERA-Interim PWV. Infact, this was found to be the case from comparison of ERA-Interim precipitation which exhibit small wet bias over Rift Valley and adjoining regions as compared to large wet bias over the central Ethiopian highlands (Mengistu Tsidu, 2012). To understand why the ERA-Interim exhibit dry bias at this site with respect to GPS PWVs, it is important to understand the climate of Nazerate and surrounding areas. Nazerate is located in the Rift Valley regions at the upper Awash river basin which is characterized by humid and high temperature as compared to dry surrounding central highlands of Ethiopia. Moreover, presence of Koka dam and sugarcane plantation in the surrounding areas could serve as a source of moisture through direct evapouration and evapotranspiration from the planation and forest from Awash National Park.

On the other hand, the general ERA-Interim trend of overestimation over highlands (e.g., at Robe (third row-left), Alamaya (bottom-right) and Mekele (bottom-left)) and

AMTD
7, 9869–9915, 2014

underestimation over lowlands (e.g., Arbaminch (third row-right) with exception of Semera) is common at these sites. Apart from the topographic features that influence reanalysis, there should be other factors that contribute to the discrepancies. For instance, Bahir Dar is located in the Ethiopian Northern highlands where ERA-Interim should have exhibited wet bias. However, as shown in Fig. 8 (second row-left) ERA-Interim shows dry bias with respect to GPS PWV. This unexplained feature in line with our previous argument can not be attributed to inaccuracy in GPS PWV since observed surface pressure is used. This means that GPS PWV is reliable as noted in our previous analysis in Sect. 3.2 and from other investigation elsewhere. The high GPS PWVs is therefore a truth that might be explained by other factors. Bahir Dar GPS site is located near Lake Tana on its southward side, largest highland lake in the region. The high evapouration rate from the water body must be responsible for the detected high PWVs. This is also the case for Arbaminch GPS site as it is located between two Rift Valley lakes on its eastern side (Lake Abaya to the north and Lake Chamo to the south) and the national park. Moreover, Lake Turkana is located far away on its southwestern side from which moisture is advected into southern part of Ethiopian Rift Valley regions by the Turkana low level jet. The boundaries of this lake and others over Ethiopia are shown by black contour lines in Fig. 1, left panels. We need to note that the smaller lakes appear in the map as dot due to the scale. However, we would like to underline that the GPS PWV is determined using GPT surface pressure in this case and the role of uncertainty in GPS PWV due to uncertainty in surface pressure could have some contribution to the over all discrepancies between ERA-Interim and GPS PWVs. Figure 9 summarizes the correlation (left) and bias (right) between ERA-Interim and GPS PWVs for all eight stations. The station labels on the horizontal axis are as described in the figure caption and also as given in Table 2. GPS and ERA-Interim are well correlated at all stations. With the exception of the three GPS sites discussed above, ERA-interim shows wet bias over GPS PWV.

AMTD
7, 9869–9915, 2014

3.4 Characterization of ERA-Interim and GPS PWVs as a function of seasons

We have noted so far that the variation in biases in ERA-Interim PWV due to local features such as proximity of GPS sites to water bodies and natural vegetation which are not resolved by large scale model such as ECMWF reanalysis model as well as inherent common model imperfection on the convection schemes used. All these factors are expected to show marked seasonal variability implying ERA-Interim performance exhibit similar features. Figure 10 shows the correlation (left) and bias (right) of ERA-Interim PWV with respect to GPS PWVs for spring (MAM), summer (JJA), autumn (SON) and winter (DJF) seasons separately as labeled on top of each panel. The correlations of ERA-Interim and GPS are generally good in the order 0.8 or greater for most sites during MAM, SON and DJF seasons. These seasons experience relatively weaker solar insolation and as a result dry to moderate humid atmosphere prevails over the region. Moreover, the southern half of the country gets moderate rainfall during MAM and SON seasons. Therefore, the variability in PWV on a daily basis does not cover wider range of values. In contrast, the correlations during wet and warm JJA summer season are mostly lower than 0.8. These features imply deficiency in the ECMWF convection schemes as indicated earlier since convection is the main source of moisture in the atmosphere. This line of reasoning is also consistent with wet bias (as shown in left panels of Fig. 10) in JJA for most of the GPS sites. While the seasonal variation in PWVs is externally forced due to solar cycle as captured correctly by both ERA-Interim and GPS (see Fig. 11), the variation in the level of agreement between the two datasets are mainly driven by the model skill in addition to the role of local features discussed in Sect. 3.3.

The seasonal cycles (Fig. 11) are well captured by all data sets. The silent features of the comparison between measurements in previous sections are well evident on a seasonal basis as well. What is perhaps important to note on the seasonal basis is the presence of large discrepancy between ERA-Interim and GPS PWVs in most

AMTD
7, 9869–9915, 2014

of wet months from May to September. In contrast, the agreements improve during relative dry months.

The role of local features such as the proximity to moisture sources and variability in the extent of this influence from season to season can be further appreciated from inspection of the vertically integrated moisture flux shown in Fig. 12. Figure 12 shows seasonal mean vertically integrated moisture (vectors) and PWV (color shade) from ERA-Interim for the 2007–2011 period of our investigation. The ERA-Interim PWV (color shade) for all seasons shows generally dry Ethiopian highlands, wet lowlands in the West and South of the country, as well as over Red Sea in the Northeast. However, there are some differences in both the seasonal mean PWV and direction of moisture transport from one season to the other. Since the vertical integration extends to 500 hPa level, this fairly represents moisture transport in the lower troposphere. For example, most of the GPS stations with exception of Mekele and Semera in the North and Northeast are under the influence of westerly and southwesterly vertically integrated moisture flux during MAM season as shown in Fig. 12a. The south western part of Ethiopia lying west of these GPS sites receives rainfall during MAM, JJA, and SON. Moreover, the region is covered by relatively dense forest. This suggests that all of the GPS sites, with the exception of Mekele and Semera in the far North and Northeast, receive moisture from this part of the country and the adjacent lakes due to the prevailing winds during MAM and SON as shown in Fig. 12a and c. The southwestern Ethiopian lowlands and adjoining eastern Sudan are also source of moisture for southern half of the country in DJF months (see Fig. 12d).

In JJA months, the moisture source in southwestern Ethiopian lowlands and adjoining eastern Sudan shifted slightly towards northwest of the country implying the GPS sites in the northern part of the country should benefit from the local moisture source due to convective rainfall (see Fig. 12b). The Red Sea region serves also as a moisture source during MAM (Fig. 12a) and DJF (Fig. 12d) as indicated by northerly and northwesterly moisture flux vectors. This is also evident from the GPS observations (see Table 4) that exhibit high PWV for Semera GPS site during these seasons as

AMTD
7, 9869–9915, 2014

compared to other GPS sites with the exception of Arbaminch. In fact, the variability in mean GPS PWVs in Table 4 from season to season are consistent with the vertically integrated moisture flux computed from ERA-Interim reanalysis. This is in clear contrast to PWV from ERA-Interim reanalysis which captures broad features due to topographic differences but not localized differences between GPS sites that arise due to proximity to water mass and vegetation cover (see Sect. 3.3) as revealed in GPS observations.

4 Conclusions

We have investigated the quality and consistency of different observational and reanalysis PWV datasets, and characterized the different error sources impacting the data taken over Addis Ababa. Upon establishing confidence in the reliability and robustness of the data from this investigation, we extended the analysis to include seven other GPS sites using GPS and ERA-Interim PWVs. This effort is aimed at filling the observational data and knowledge gaps regarding water vapour variability in this part of the globe for the first time.

The PWVs from GPS and FTIR are characterized in terms of different sources of error. Some reprocessing are also undertaken to assess the level of propagated uncertainty in PWVs. For example, the surface pressure in the pressure profile used in retrieval of water vapour VMR from FTIR spectra is replaced with synoptic surface pressure observations at the Addis Ababa FTIR site during determination of PWV from VMR. The difference between the original and reprocessed PWVs is attributed to uncertainty that can arise from surface pressure uncertainty. This difference is found to be negligible. Moreover, the propagated uncertainty from statistical and systematic formal retrieval error is also found to be very small. The GPS PWV is sensitive to uncertainty in surface pressure in general. However, the magnitude and sign of correction of PWVs made using observed surface pressure at four GPS stations are different from station to station. As a result, the gain obtained from use of observed surface pressure in terms of reducing bias and strengthening correlation is significant but shows some variations

AMTD
7, 9869–9915, 2014

among the GPS sites. This variation reveals the variation in the skill of GPT model for different part of the country and underlines the importance of surface pressure observations in PWV study from GPS observations.

The radiosonde sounding is an in-situ observation, however, most of the sensors used are known to suffer from dry bias. This is indeed the case in this intercomparison as reflected by dry bias in PWV from vaisala RS92 radiosonde with respect to ERA-Interim and GPS. Direct comparison with FTIR was not possible due to absence of coincident measurements that meet the time window of 1 h from each other. However, it can be inferred from comparison of FTIR with ERA-Interim and GPS for other coincident observations, which shows both GPS and ERA-Interim have higher wet biases in their PWV measurements than those with respect to radiosonde, that radiosonde exhibits dry bias with respect to FTIR as well.

The comparison between GPS and ERA-Interim PWVs over seven other GPS stations shows difference in the magnitude and sign of bias of ERA-Interim with respect to GPS PWV from station to station. This variation is also visible across different seasons. The main cause of the variation is linked to variation in model skill over different regions and seasons. From previous similar as well as indirect studies related with precipitation, the model convection scheme is sensitive to topographic variation. ECMWF ERA-Interim tends to show wet precipitation bias over highlands and dry bias over lowlands. The GPS and ERA-Interim PWV exhibit similar sensitivity to topographic differences. However, there are also other factors such as proximity to water bodies in the case of PWVs that led to difference between the reanalysis and GPS PWVs. For instance, the presence of Lake Tana near the northern highland GPS station at Bahir Dar led to wet bias in GPS PWV with respect to ERA-Interim contrary to the general tendency of high precipitation and PWVs in ECMWF reanalysis model. This is also the case at Arbaminch GPS station located between two lakes, though the model is expected to show dry bias in this case regardless of the lakes in the same direction. The skill of ECMWF in reproducing realistic PWV varies with season showing large bias during wet summer and dry winter months. The good agreement as characterized

AMTD
7, 9869–9915, 2014

by correlation between GPS and ERA-Interim PWVs is achieved during spring (MAM), autumn (SON) and winter (DJF) months at all stations.

In summary, the intercomparison of different instruments and reanalysis over this region is the first step towards bridging data and knowledge gaps of the global water vapour variability created due to lack of observational infrastructure in this part of the world in the past. The study will serve as starting point from which further studies will be conducted with respect to validation of satellite products, understanding water vapour budget and dynamics governing it.

Acknowledgements. The authors acknowledge NOAA NCDC for radiosonde and surface pressure data, UNAVCO for installation, maintainance and free access to GPS data, and ECMWF for access to ERA-Interim data sets. The first author would also like to acknowledge the financial support of the Humboldt foundation through the author's Humboldt fellowship grant during which this work is accomplished. We acknowledge support by Deutsche Forschungsgemeinschaft and Open Access Publishing Fund of the Karlsruhe Institute of Technology.

The service charges for this open access publication have been covered by a Research Centre of the Helmholtz Association.

References

Agusti-Panareda, A., Vasiljevic, D., Beljaars, A., Bock, O., Guichard, F., Nuret, M., Mendez, A. G., Andersson, E., Bechtold, P., Fink, A., Hersbach, H., Lafore, J.-P., Ngamini, J.-B., Parker, D. J., Redelsperger, J.-L., and Tomkins, A. M.: Radiosonde humidity bias correction over the West African region for the special AMMA reanalysis at ECMWF, Q. J. Roy. Meteor. Soc., 135, 595–617, doi:10.1002/qj.396, 2009. 9883

Auligne, T., McNally, A., and Dee, D.: Adaptive bias correction for satellite data in a numerical weather prediction system, Q. J. Roy. Meteor. Soc., 133, 631–642, 2007. 9884

Bevis, M., Businger, S., Herring, T. A., Rocken, C., Anthes, R. A., and Ware, R. H.: GPS meteorology-Remote-sensing of atmospheric water-vapor using the Global Positioning System, J. Geophys. Res., 97, 15787–15801, 1992. 9873, 9881

AMTD
7, 9869–9915, 2014

Bevis, M., Businger, S., Chiswell, S., Herring, T. A., Anthes, R. A., Rocken, C., and Ware, R. H.: GPS meteorology – mapping zenith wet delays onto precipitable water, J. Appl. Meteorol., 33, 379–386, 1994. 9873, 9877

Bock, O., Keil, C., Richard, E., Flamant, C., and Bouin, M.-N.: Validation of precipitable water from ECMWF model analyses with GPS and radiosonde data during the MAP SOP, Q. J. Roy. Meteor. Soc., 131, 3013–3036, doi:10.1256/qj.05.27, 2005. 9875

Bock, O., Bouin, M. N., Walpersdorf, A., Lafore, J. P., Janicot, S., Guichard, F., and Agusti-Panareda, A.: Comparison of ground-based GPS precipitable water vapour to independent observations and NWP model reanalyses over Africa, Q. J. Roy. Meteor. Soc., 133, 2011–2027, 2007. 9873, 9874, 9875, 9879, 9880, 9881

Bock, O., Bouin, M. N., Doerflinger, E., Collard, P., Masson, F., Meynadier, R., Nahmani, S., Koité, M., Gaptia Lawan Balawan, K., Didé, F., Ouedraogo, D., Pokperlaar, S., Ngamini, J.-B., Lafore, J. P., Janicot, S., Guichard, F., and Nuret, M.: West African Monsoon observed with ground-based GPS receivers during African Monsoon Multidisciplinary Analysis (AMMA), J. Geophys. Res., 113, 1–53, 2008. 9881

Bock, O., Willis, P., Lacarra, M., and Bosser, P.: An inter-comparison of zenith tropospheric delays derived from DORIS and GPS data, Adv. Space Res., 46, 1648–1660, 2010. 9873

Boehm, J., Heinkelmann, R., and Schuh, H.: Short note: a global model of pressure and temperature for geodetic applications, J. Geod., 81, 679–683, 2007. 9877, 9878

Braun, J., Rocken, C., and Liljegren, C.: Comparisons of line-of-sight water vapor observations using the global positioning system and a pointing microwave radiometer, J. Atmos. Ocean. Tech., 20, 606–612, 2003. 9873

Buehler, S. A., von Engeln, A., Brocard, E., John, V. O., Kuhn, T., and Eriksson, P.: Recent developments in the line-by-line modeling of outgoing longwave radiation, J. Quant. Spectrosc. Ra., 98, 446–457, doi:10.1016/j.jqsrt.2005.11.001, 2006. 9871

Buehler, S. A., Östman, S., Melsheimer, C., Holl, G., Eliasson, S., John, V. O., Blumenstock, T., Hase, F., Elgered, G., Raffalski, U., Nasuno, T., Satoh, M., Milz, M., and Mendrok, J.: A multi-instrument comparison of integrated water vapour measurements at a high latitude site, Atmos. Chem. Phys., 12, 10925–10943, doi:10.5194/acp-12-10925-2012, 2012. 9873

Champollion, C., Masson, F., Bouin, M.-N., Walpersdorf, A., Doerflinger, E., Bock, O., and Van Baelen, J.: GPS water vapour tomography: preliminary results from the ESCOMPTE field experiment, Atmos. Res., 74, 253–274, 2005. 9873

AMTD
7, 9869–9915, 2014

Combrink, A., Combrinck, W., and Moraal, H.: Near real-time detection of atmospheric water vapour using the SADC GPS network, S. Afr. J. Sci., 100, 436–442, 2004. 9873

Dai, A., Wang, J., Ware, R. H., and Hove, T. V.: Diurnal variation in water vapor over North America and its implications for sampling errors in radiosonde humidity, J. Geophys. Res., 107, 4090, doi:10.1029/2001JD000642, 2002. 9872

Dee, D. P., Uppala, S. M., Simmons, A. J., Berrisford, P., Poli, P., Kobayashi, S., Andrae, U., Balmaseda, M. A., Balsamo, G., Bauer, P., Bechtold, P., Beljaars, A. C. M., van de Berg, L., Bidlot, J., Bormann, N., Delsol, C., Dragani, R., Fuentes, M., Geer, A. J., Haimberger, L., Healy, S. B., Hersbach, H., Hólm, E. V., Isaksen, L., Kållberg, P., Köhler, M., Matricardi, M., McNally, A. P., Monge-Sanz, B. M., Morcrette, J.-J., Park, B.-K., Peubey, C., de Rosnay, P., Tavolato, C., Thépaut, J.-N., and Vitart, F.: The ERA-Interim reanalysis: configuration and performance of the data assimilation system, Q. J. Roy. Meteor. Soc., 137, 553–597, doi:10.1002/qj.828, 2011. 9879, 9883

Dietrich, S. V. R., Johnsen, K.-P., Miao, J., and Heygster, G.: Comparison of tropospheric water vapour over Antarctica derived from AMSU-B data, ground-based GPS data and the NCEP/NCAR reanalysis, J. Meteorol. Soc. Jpn., 82, 259–267, 2004. 9873

Durre, I., Vose, S. R., and Wuertz, D. B.: Overview of the Integrated Global Radiosonde Archive, J. Climate, 19, 53–68, 2006. 9879, 9883

Fetzer, E., McMillin, L. M., Tobin, D., Aumann, H. H., Gunson, M. R., McMillan, W. W., Hagan, D. E., Hofstadter, M. D., Yoe, J, Whiteman, D. N., Barnes, J. E., Bennartz, R., Vömel, H., Walden, V., Newchurch M., Minnett, P. J., Atlas, R., Schmidlin, F., Olsen, E. T., Goldberg, M. D., Zhou, S., Ding, H., Smith, W. L., and Revercomb, H.: AIRS/AMSU/HSB Validation, IEEE T. Geosci. Remote, 4, 418–431, 2003. 9873

Gendt, G., Dick, G., Reigber, C., Tomassini, M., Liu, Y., and Ramatschi, M.: Near real time GPS water vapor monitoring for numerical weather prediction in Germany, J. Meteorol. Soc. Jpn., 82, 361–370, 2004. 9873

Gradinarsky, L. P., Johansson, J. M., Bouma, H. R., Scherneck, H.-G., and Elgered, G.: Climate monitoring using GPS, Phys. Chem. Earth, 27, 335–340, 2002. 9873

Guerova, G., Brockmann, E., Quiby, J., Schubiger, F., and Matzler, C.: Validation of NWP mesoscale models with Swiss GPS network AGNES, J. Appl. Meteorol., 42, 141–150, 2003. 9873

AMTD
7, 9869–9915, 2014

Hase, F., Blumenstock, T., and Paton-Walsh, C.: Analysis of the instrumental line shape of high-resolution Fourier transform IR spectrometers with gas cell measurements and new retrieval software, Appl. Optics, 38, 3417–3422, 1999. 9876

King, M. D. W., Menzel, P., Kaufman, Y. J., Tanré, D., Gao, B.-C., Platnick, S., Ackerman, S. A., Remer, L. A., Pincus, R., and Hubanks, P. A.: Cloud and Aerosol Properties, Precipitable Water, and Profiles of Temperature and Water Vapor from MODIS, IEEE T. Geosci. Remote, 41, 442–458, 2003. 9873

King, R. and Bock, Y.: Documentation of the GAMIT GPS Analysis Software, in: release 10.3 Edition, Massachusetts Institute of Technology and Scripts Institution of Oceanography, University of California at San Diego, 2006. 9877

Klein Baltink, H., van der Marel, H., and van der Hoeven, A. G. A.: Integrated atmospheric water vapor estimates from a regional GPS network, J. Geophys. Res., 107, ACL3.1–ACL3-8, doi:10.1029/2000JD000094, 2002. 9881

Koulali, A., Ouazar, D., Bock, O., and Fadil, A.: Study of seasonal-scale atmospheric water cycle with ground-based GPS receivers, radiosondes and NWP models over Morocco, Atmos. Res., 104–105, 273–291, doi:10.1016/j.atmosres.2011.11.002, 2011. 9874, 9875

Mears, C., Santer, B. D., Wentz, F. J., Taylor, K., and Wehner, M.: Relationship between temperature and precipitable water changes over tropical oceans, Geophys. Res. Lett., 34, L24709, doi:10.1029/2007GL031936, 2007. 9871

Mengistu Tsidu, G.: High-resolution monthly rainfall database for Ethiopia: homogenization, reconstruction, and gridding, J. Climate, 25, 8422–8443, 2012. 9878, 9884, 9885, 9888

Miloshevich, L. M., Vomel, H., Whiteman, D., Lesht, B., Schmidlin, F., and Russo, F.: Absolute accuracy of water vapor measurements from six operational radiosonde types launched during AWEX-G and implication of AIRS validation, J. Geophys. Res., 111, D09S10, doi:10.1029/2005JD006083, 2006. 9883

Nilsson, T. and Elgered, G.: Long-term trends in the atmospheric water vapor content estimated from ground-based GPS data, J. Geophys. Res., 113, D19101, doi:10.1029/2008JD010110, 2008. 9871

Ning, T., Elgered, G., Willen, U., and Johansson, J. M.: Evaluation of the atmospheric water vapor content in a regional climate model using ground-based GPS measurements, J. Geophys. Res., 118, 329–339, doi:10.1029/2012JD018053, 2013. 9881

AMTD
7, 9869–9915, 2014

Paul Berrisford, P., Dee, D., Fielding, K., Fuentes, M., Kollberg, P., Kobayashi, S., and Uppala, S.: The ERA-Interim archive Version 1.0 Series: ERA Report Series, ECMWF, Shinfield Park, Reading, Berkshire RG2 9AX, UK, 2009. 9883

Rocken, C., Ware, R. H., Hove, T. V., Solheim, F., Alber, C., and Johnson, J.: Sensing atmospheric water vapor with the Global Positioning System, Geophys. Res. Lett., 20, 2631–2634, 1993. 9873

Rocken, C., Hove, T. V., and Ware, R. H.: Near real-time GPS sensing of atmospheric water vapor, Geophys. Res. Lett., 24, 3221–3224, 1997. 9873

Rodgers, C. D.: Retrieval of atmospheric temperature and composition from remote measurements of thermal radiation, Rev. Geophys., 14, 609–624, 1976. 9876

Rodgers, C. D.: Inverse Methods for Atmospheric Sounding – Theory and Practise, Vol. 2, World Scientific, Series on Atmospheric, Oceanic and Planetary Physics, 2000. 9876, 9881

Saastamoinen, J.: Atmospheric correction for the troposphere and stratosphere in radio ranging of satellites, in: Geophys. Monogr. Ser. 15, edited by: Henriksen, S. W., 247–251, 1972. 9876

Schneider, M., Hase, F., and Blumenstock, T.: Water vapour profiles by ground-based FTIR spectroscopy: study for an optimised retrieval and its validation, Atmos. Chem. Phys., 6, 811–830, doi:10.5194/acp-6-811-2006, 2006. 9881

Schneider, M., Romero, P. M., Hase, F., Blumenstock, T., Cuevas, E., and Ramos, R.: Continuous quality assessment of atmospheric water vapour measurement techniques: FTIR, Cimel, MFRSR, GPS, and Vaisala RS92, Atmos. Meas. Tech., 3, 323–338, doi:10.5194/amt-3-323-2010, 2010. 9873, 9886

Schneider, M., Barthlott, S., Hase, F., González, Y., Yoshimura, K., García, O. E., Sepúlveda, E., Gomez-Pelaez, A., Gisi, M., Kohlhepp, R., Dohe, S., Blumenstock, T., Wiegele, A., Christner, E., Strong, K., Weaver, D., Palm, M., Deutscher, N. M., Warneke, T., Notholt, J., Lejeune, B., Demoulin, P., Jones, N., Griffith, D. W. T., Smale, D., and Robinson, J.: Ground-based remote sensing of tropospheric water vapour isotopologues within the project MUSICA, Atmos. Meas. Tech., 5, 3007–3027, doi:10.5194/amt-5-3007-2012, 2012. 9875, 9880

Takele Kenea, S., Mengistu Tsidu, G., Blumenstock, T., Hase, F., von Clarmann, T., and Stiller, G. P.: Retrieval and satellite intercomparison of O_3 measurements from ground-based FTIR Spectrometer at Equatorial Station: Addis Ababa, Ethiopia, Atmos. Meas. Tech., 6, 495–509, doi:10.5194/amt-6-495-2013, 2013. 9875, 9881

AMTD
7, 9869–9915, 2014

Trenberth, K. E., Fasullo, J., and Smith, L.: Trends and variability in column-integrated atmospheric water vapor, Clim. Dynam., 241, 741–758, doi:10.1007/s00382-005-0017-4, 2005. 9883

Turner, D., Lesht, B. M., Clough, S., Liljegren, J., Revercomb, H., and Tobin, D.: Dry bias and variability in Vaisala RS80-H radiosondes: the ARM experience, J. Atmos. Ocean. Tech., 20, 117–132, 2003. 9883

Van Baelen, J., Aubagnac, J.-P., and Dabas, A.: Comparison of near-real time estimates of integrated water vapor derived with GPS, radiosondes, and microwave radiometer, J. Atmos. Ocean. Tech., 22, 201–210, 2005. 9873

Vedel, H. and Huang, X.-Y.: Impact of ground based GPS data on numerical weather prediction, J. Meteorol. Soc. Jpn., 82, 459–472, 2004. 9873

Vedel, H., Huang, X.-Y., Haase, J., Ge, M., and Calais, E.: Impact of GPS zenith tropospheric delay data on precipitation forecasts in Mediterranean France and Spain, Geophys. Res. Lett., 31, L02102, doi:10.1029/2003GL017715, 2004. 9873

Voemel, H., Selkirk, H., Miloshecich, L., Valverde-Canossa, J., Valdes, J., Kyro, E., Kivi, R., Stolz, W., Peng, G., and Diaz, A.: Radiation dry bias of the VaisalaRS92 humidity sensor, J. Atmos. Ocean. Tech., 24, 953–963, 2007. 9883

Wang, J., Zhang, L., Dai, A., Hove, T. V., and Baelen, J. V.: A near-global, 2 hourly data set of atmospheric precipitable water from ground-based GPS measurements, J. Geophys. Res., 112, D11107, doi:10.1029/2006JD007529, 2007. 9872, 9873, 9882

Wang, Y., Liu, Y., Liu, L., Guo, Z., Ge, X., and Xu, H.: Retrieval of the change of precipitable water vapor with zenith tropospheric delay in the Chinese mainland, Adv. Space Res., 43, 82–88, 2009. 9873

Yang, X. H., Sass, B. H., Elgered, G., Johansson, J. M., and Emardson, T. R.: A comparison of precipitable water vapor estimates by an NWP simulation and GPS observations, J. Appl. Meteorol., 38, 941–956, 1999. 9873

Zeleke, T., Giorgi, F., Tsidu, G. M., and Diro, G. T.: Spatial and temporal variability of summer rainfall over Ethiopia from observations and a regional climate model experiment, Theor. Appl. Climatol., 111, 665–681, doi:10.1007/s00704-012-0700-4, 2013. 9885

AMTD
7, 9869–9915, 2014

Table 1. The spectral microwindows used for retrieval of water vapour and major interfering species considered.

Microwindow (cm^{-1})	interfering species
2659.0–2661.0	HDO, O_3, CH_4, HCl, C_2H_6
2662.0–2664.2	
2665.8–2666.8	
2677.2–2678.2	
2974.2–2975.6	
2983.1–2985.2	
2991.0–2996.0	

AMTD
7, 9869–9915, 2014

Table 2. The ground-based GPS receivers used in this study and their geocoordinates.

Station	short name	Longitude (°)	Latitude (°)	Altitude (m)
Addis Ababa*	Add	38.7606	9.0298	2438.9409
Alemaya	Ale	42.0339	9.3609	2042.3094
Arbaminch	Arb	37.5609	9.0298	1199.8563
Bahir Dar*	Bah	37.3597	11.5243	1793.1231
Semera	Sem	41.0092	11.7019	418.3076
Nazerate*	Naz	39.2906	8.5112	1722.6016
Robe	Rob	40.0261	7.0663	2458.1883
Mekele*	Mek	39.4828	13.3939	2226.0376

* GPS stations for which surface observation is available.

AMTD
7, 9869–9915, 2014

Table 3. The observation periods covered in the study. Presence of data gaps, which differ from station to station, implies less number of observations are considered in the study than what the coverge period in the table suggests as will be shown later in Sect. 3.

Station	FTIR	GPS	Radiosonde	ERA-Interim
Addis Ababa	2009–2011	2007–2011	2007–2011	2007–2011
Alemaya		2007–2009		2007–2011
Arbaminch		2007–2011		2007–2011
Bahir Dar		2007–2011		2007–2011
Semera		2007–2009		2007–2011
Nazerate		2007–2011		2007–2011
Robe		2007–2009		2007–2011
Mekele		2008		2007–2011

AMTD
7, 9869–9915, 2014

Table 4. The seasonal mean PWV (mm) as determined from the 8 ground-based GPS receivers used in this study.

Station	MAM	JJA	SON	DJF
Addis Ababa	18.45	25.04	19.80	15.46
Alemaya	19.70	26.52	20.66	14.92
Arbaminch	31.96	35.55	33.35	25.50
Bahir Dar	22.12	32.28	26.40	16.94
Semera	25.44	31.76	29.69	24.12
Nazerate	23.47	29.04	24.02	19.39
Robe	19.60	22.48	21.18	14.72
Mekele	–	24.68	17.22	11.54

AMTD
7, 9869–9915, 2014

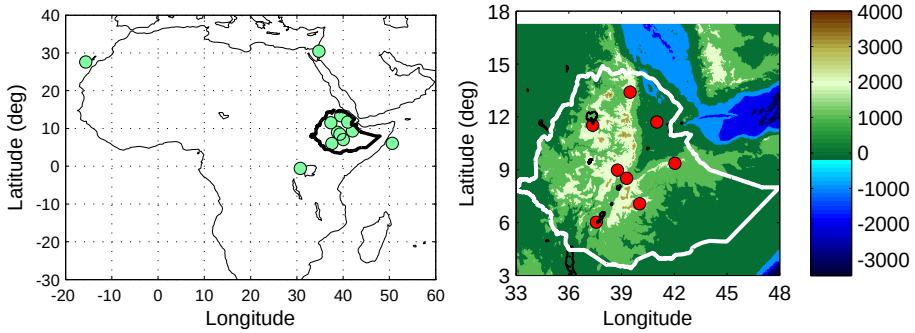

Figure 1. UNAVCO GPS ground receiver sites used in GPS solution using GAMIT software over the region (left) and locatopns of GPS receivers used in the analysis of PWV, nearby lakes and topography of the country (right).

AMTD
7, 9869–9915, 2014

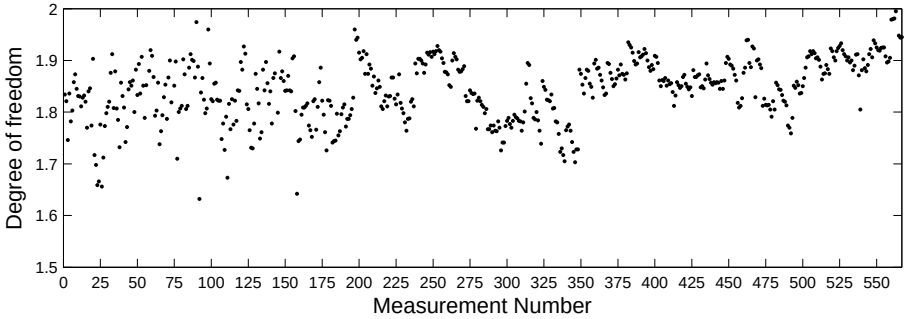

Figure 2. Degrees of freedom of signal (DOFS) for all FTIR measurements. DOFS is a dimensionless quantity and a measure of independent piece of information retrieved from measurement. It is inconvient to use x axis as time since that leads to cluster of data points from which the above variations can not be observed because of wider and large number of temporal gaps over a period of 2009 to 2011. Moreover, measurements on a given day are at close interval of few minutes to half an hour.

AMTD
7, 9869–9915, 2014

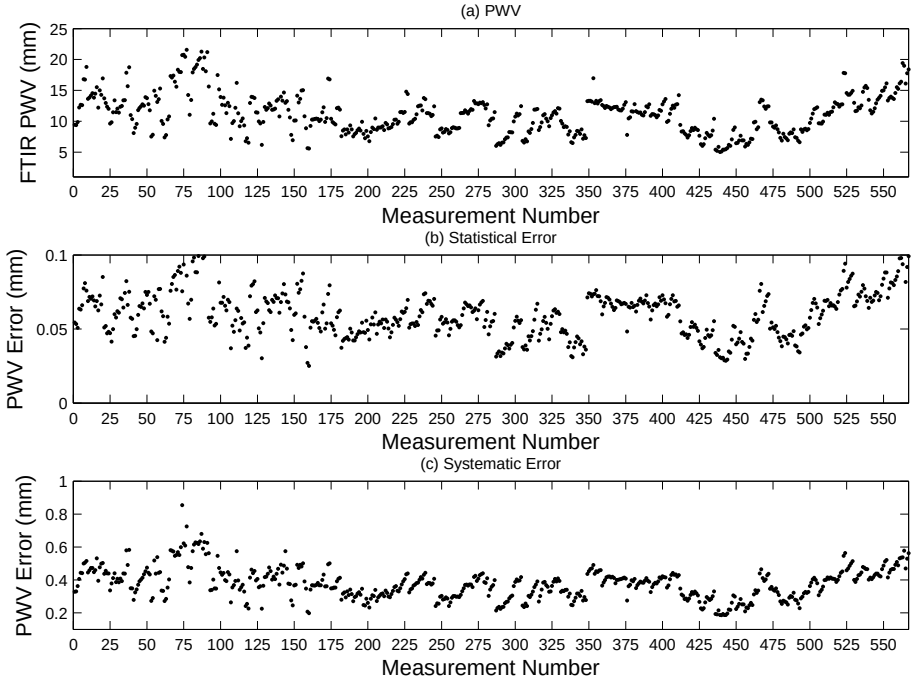

Figure 3. FTIR observations: **(a)** PWV; **(b)** Statistical error due to random retrieval errors in water vapour column; and **(c)** Systematic error.

AMTD
7, 9869–9915, 2014

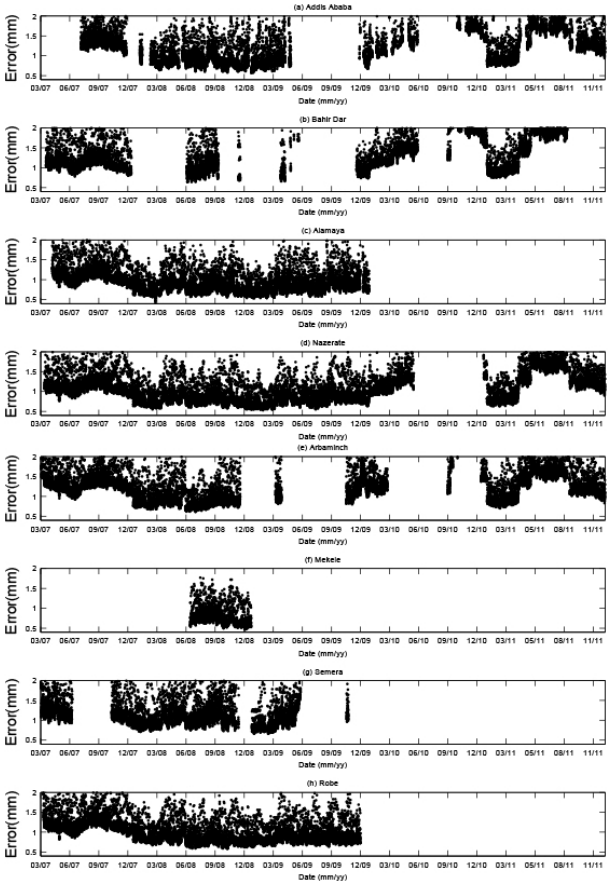

Figure 4. Formal GPS PWV error from GAMIT least squares solution for respective GPS station shown on top of each panel **(a)** to **(h)**. The panels are scaled to the same time axis range for the sake of comparison.

AMTD
7, 9869–9915, 2014

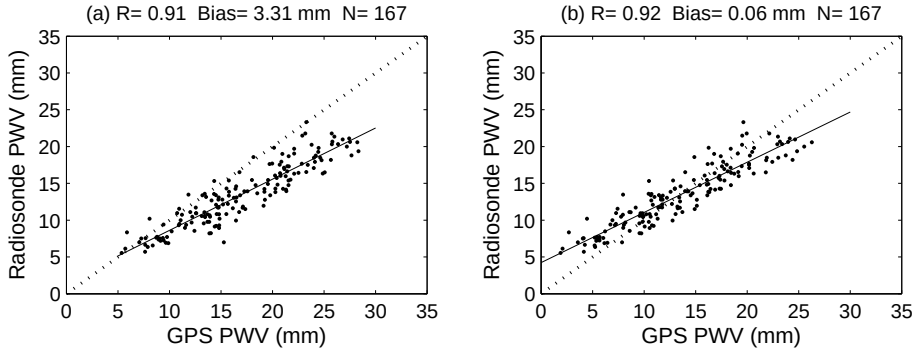

Figure 5. Comparison of GPS-drived and radiosonde PWVs at 12:00 UTC for coincident measurements when **(a)** GPT surface pressure, and **(b)** observed surface pressure is used in GPS PWV evaluations.

AMTD
7, 9869–9915, 2014

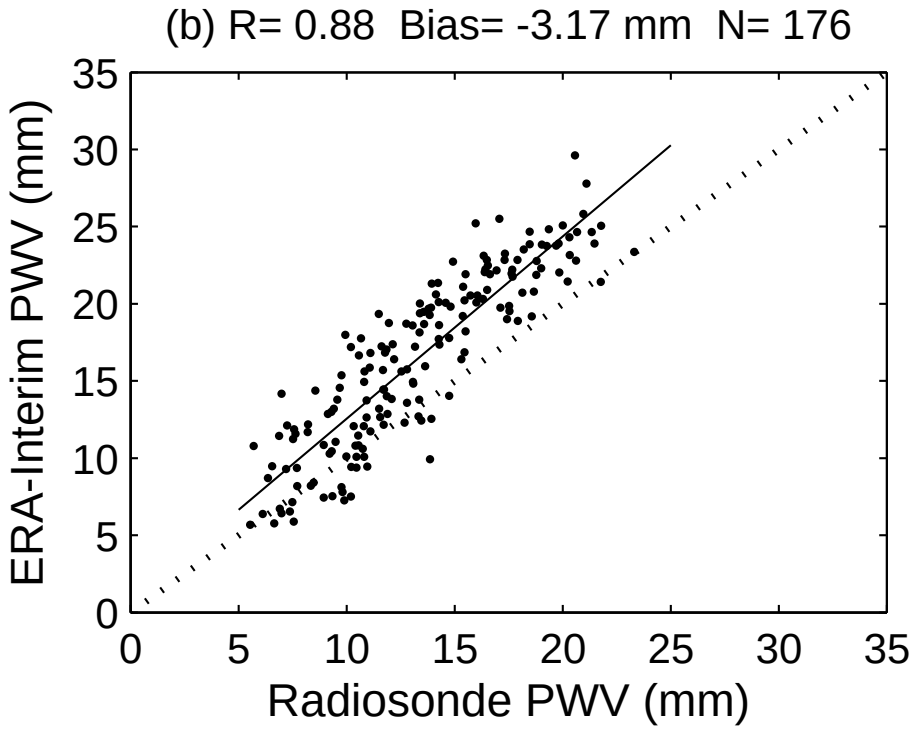

Figure 6. The same as Fig. 5 but between ECMWF ERA-Interim reanalysis and radiosonde PWVs at 12:00 UTC when altitude correction is made using Eq. (4).

AMTD
7, 9869–9915, 2014

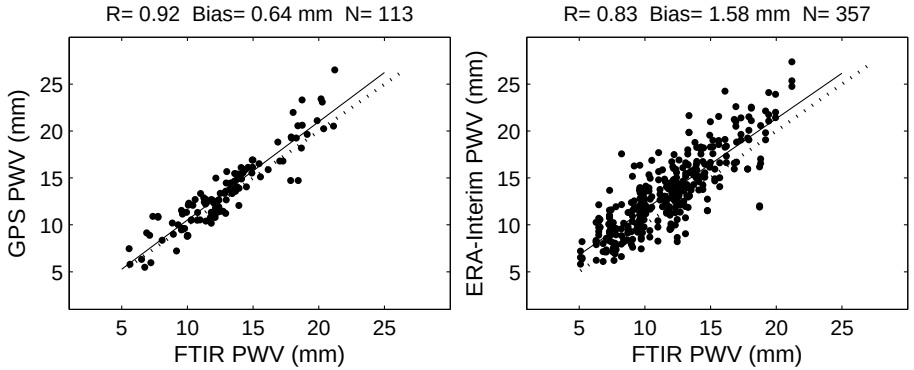

Figure 7. Comparison of GPS-drived and ECMWF ERA-Interim reanalysis PWVs with FTIR coincident measurements.

AMTD
7, 9869–9915, 2014

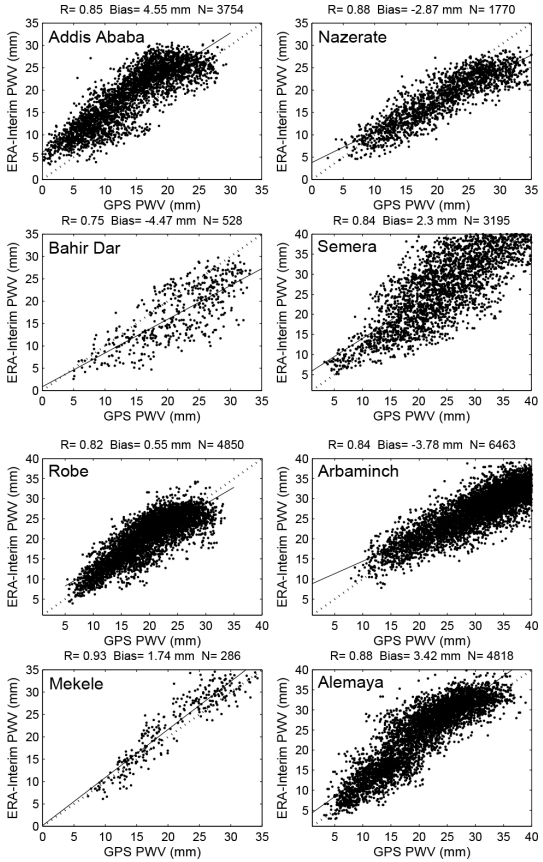

Figure 8. Comparison of GPS and ERA-Interim PWVs at 8 sites, each site is shown at left-top corner of each panel, in Ethiopia.

AMTD
7, 9869–9915, 2014

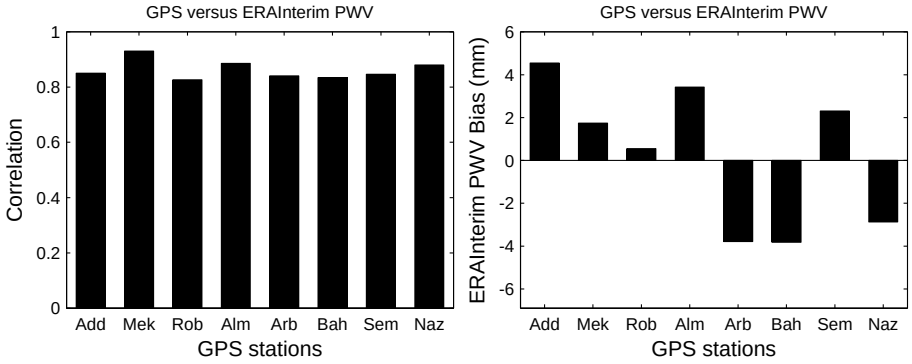

Figure 9. Correlation of individual observations between ERA-Interim and GPS (left) and bias in ERA-Interim with respect to GPS (right) for all 8 ground GPS receiver sites. From left to right on the horizontal axis: Addis Ababa (Add), Mekele (Mek), Robe (Rob), Alemaya (Alm), Arbaminch (Arb), Bahir Dar (Bah), Semera (Sem), and Nazerate (Naz).

AMTD
7, 9869–9915, 2014

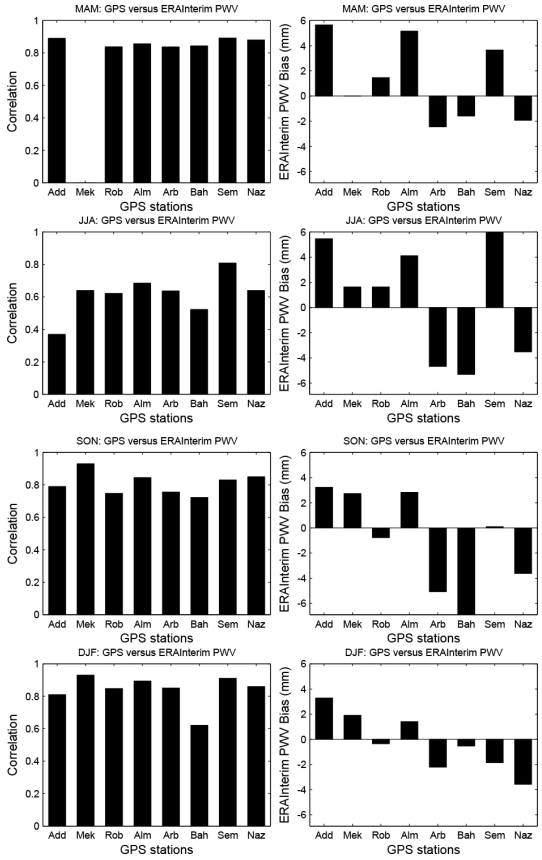

Figure 10. The same as Fig. 9 for ERA-Interim vs. GPS but separated into seasons: MAM (top row), JJA (second row), SON (third row) and DJF (last row).

AMTD
7, 9869–9915, 2014

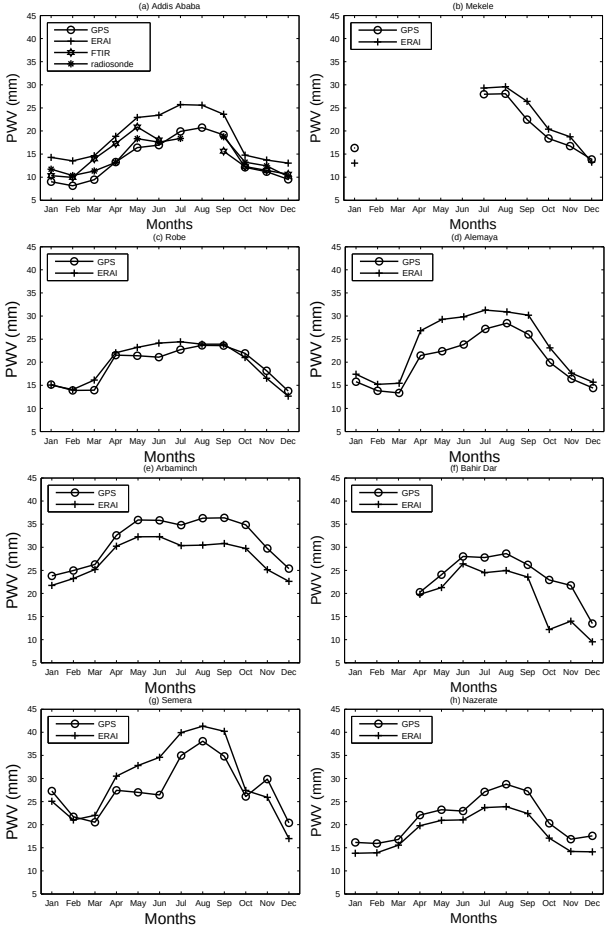

Figure 11. The seasonal water vapour cycle as captured by different data sets.

AMTD
7, 9869–9915, 2014

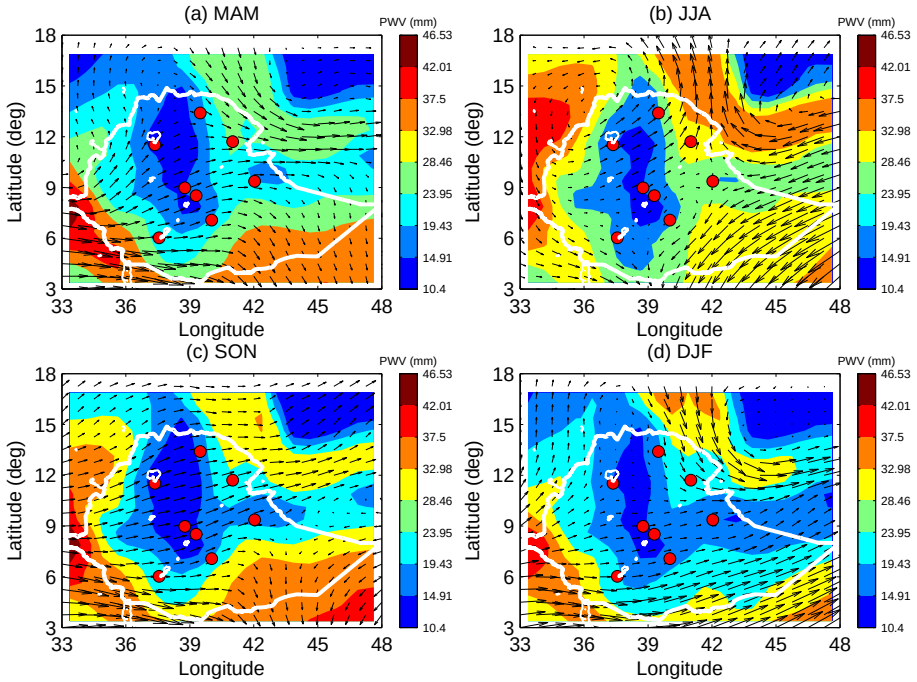

Figure 12. The ECMWF PWV (color contour), and vertically integrated moisture flux (vectors).

AMTD
7, 9869–9915, 2014